Engineered protein disaggregases mitigate toxicity of aberrant prion-like fusion proteins underlying sarcoma

Received for publication, May 22, 2019, and in revised form, May 30, 2019 Published, Papers in Press, June 5, 2019, DOI 10.1074/jbc.RA119.009494

Jeremy J. Ryan[‡], **Macy L. Sprunger**[‡], **Kayla Holthaus**[‡], **James Shorter**[§1], **and Meredith E. Jackrel**[‡2]

From the [‡]*Department of Chemistry, Washington University, St. Louis, Missouri 63130 and* [§]*Department of Biochemistry and Biophysics, Perelman School of Medicine, University of Pennsylvania, Philadelphia, Pennsylvania 19104*

Edited by Paul E. Fraser

FUS and EWSR1 are RNA-binding proteins with prion-like domains (PrLDs) that aggregate in amyotrophic lateral sclerosis (ALS) and frontotemporal dementia (FTD). The *FUS* and *EWSR1* genes are also prone to chromosomal translocation events, which result in aberrant fusions between portions of the PrLDs of FUS and EWSR1 and the transcription factors CHOP and FLI. The resulting fusion proteins, FUS-CHOP and EWS-FLI, drive aberrant transcriptional programs that underpin liposarcoma and Ewing's sarcoma, respectively. The translocated PrLDs alter the expression profiles of these proteins and promote their phase separation and aggregation. Here, we report the development of yeast models of FUS-CHOP and EWS-FLI toxicity and aggregation. These models recapitulated several salient features of sarcoma patient cells harboring the FUS-CHOP and EWS-FLI translocations. To reverse FUS and EWSR1 aggregation, we have explored Hsp104, a hexameric AAA+ protein disaggregase from yeast. Previously, we engineered potentiated Hsp104 variants to suppress the proteotoxicity, aggregation, and mislocalization of FUS and other proteins that aggregate in ALS/FTD and Parkinson's disease. Potentiated Hsp104 variants that robustly suppressed FUS toxicity and aggregation also suppressed the toxicity and aggregation of FUS-CHOP and EWS-FLI. We suggest that these new yeast models are powerful platforms for screening for modulators of FUS-CHOP and EWS-FLI phase separation. Moreover, Hsp104 variants might be employed to combat the toxicity and phase separation of aberrant fusion proteins involved in sarcoma.

Chromosomal translocation events underpin sarcoma (1). In liposarcoma, the N-terminal portion of FUS[3] becomes aberrantly fused to the transcription factor CHOP (1). In Ewing's sarcoma, the second most common pediatric bone cancer, a chromosomal translocation event inappropriately fuses the N-terminal region of EWSR1 to the transcription factor FLI (1). The EWS-FLI translocation can occur in multiple frames, leading to the formation of different translocation products (1). Due to their fusion to portions of FUS and EWSR1, the transcription factors become differentially regulated and elicit aberrant transcriptional programs (1). For instance, FLI is expressed only under specific conditions, whereas EWSR1 is constitutively expressed (1). Fusion of FLI to EWSR1 results in constitutive expression of FLI in the form of the EWS-FLI fusion. Both FUS and EWSR1 harbor prion-like domains (PrLDs), and large portions of these PrLDs are retained in the translocated products (1, 2). PrLDs are found in ~240 human proteins and resemble yeast prion domains in their aggregation propensity and precise low-complexity amino acid composition, which is enriched for uncharged polar residues and glycine (3–6). The PrLDs of FUS and EWSR1 drive the aggregation and toxicity of full-length FUS and EWSR1, which aggregate in subsets of patients with amyotrophic lateral sclerosis (ALS) or frontotemporal dementia (FTD) (7–13). Thus, in addition to altered expression profiles, the PrLDs of FUS and EWSR1 may dramatically alter the biochemical properties of CHOP and FLI (2, 12). In fact, the PrLD of EWS-FLI promotes aberrant phase separation events, which lead to the inappropriate recruitment of chromatin-remodeling factors, activating the deleterious transcriptional events of Ewing's sarcoma (2). Thus, agents that antagonize these aberrant phase separation events could be therapeutic for sarcoma (2, 14–16).

To study human disease in a highly genetically tractable model system, we and others have demonstrated that diverse protein-misfolding disorders can be modeled in the budding yeast, *Saccharomyces cerevisiae* (7–9, 17–24). Excellent models have been developed for studying FUS and EWSR1 misfolding (in ALS/FTD) as well as α-synuclein (in Parkinson's disease) and TDP-43 (in ALS/FTD) among others (7–9, 17–24). Yeast models recapitulate many of the molecular phenotypes observed in patients with these respective disorders, and they are also highly genetically tractable platforms, which enable rapid screening for genetic and small-molecule modifiers (7, 17–19, 21, 23–26). For instance, the RNA-binding protein FUS shuttles to the nucleus to fulfill its roles in regulating RNA homeostasis (10). However, in ALS/FTD patients and in yeast models of FUS proteinopathy, FUS is toxic and aggregates in

This work was supported by Washington University startup funds, NIGMS, National Institutes of Health Grants R35GM128772 (to M. E. J.) and R01GM099836 (to J. S.), and an Abramson Cancer Center sarcoma pilot grant (to J. S.). The authors declare that they have no conflicts of interest with the contents of this article. The content is solely the responsibility of the authors and does not necessarily represent the official views of the National Institutes of Health.

[1] To whom correspondence may be addressed. Tel.: 215-573-4256; E-mail: jshorter@pennmedicine.upenn.edu.

[2] To whom correspondence may be addressed. Tel.: 314-935-2826; E-mail: mjackrel@wustl.edu.

[3] The abbreviations used are: FUS, fused in sarcoma; CHOP, CCAAT-enhancer–binding protein (C/EBP) homologous protein; AAA+, ATPases associated with diverse cellular activities; EWS, Ewing sarcoma; FLI, friend leukemia integration 1 transcription factor; FRAP, fluorescence recovery after photobleaching; FTD, frontotemporal dementia; GAL, galactose; Hsp, heat shock protein; PrLD, prion-like domain; RGG, arginine/glycine-rich; ROI, region of interest; RRM, RNA-recognition motif; PGK, 3-phosphoglycerate kinase.

the cytoplasm (7, 10, 11, 21). This yeast system has been used to identify potent genetic modifiers of FUS aggregation and toxicity (7, 21, 27, 28). Here, we establish yeast models for studying the aggregation of FUS-CHOP and EWS-FLI. Additionally, we assessed whether protein disaggregases that dissolve FUS aggregates might also be capable of dispersing altered FUS-CHOP and EWS-FLI phases (27, 29, 30).

Prions are not invariably toxic or harmful (31–34). In *S. cerevisiae*, prions are harnessed for adaptive purposes, and so they are tightly regulated (35, 36). The AAA+ protein Hsp104 constructs and deconstructs yeast prions and solubilizes proteins that accumulate after environmental stress (37–51). We hypothesized that the shared cross-β structure of amyloids might enable a protein that naturally regulates amyloid in yeast to be active against similarly structured proteins that underpin human disease (39, 52, 53). However, Hsp104 has somewhat limited ability to disaggregate proteins that aggregate in human disease (27, 54, 55). Thus, we have used protein engineering to potentiate Hsp104 (56). We have found that potentiated Hsp104 variants suppress the misfolding and toxicity of diverse proteins that form amyloid or harbor prion-like domains (27, 29, 57–61). Enhanced Hsp104 disaggregases suppress the toxicity of TDP-43, FUS, and α-synuclein as well as disease-associated mutants of these proteins, and they suppress toxicity under conditions where WT Hsp104 is ineffective (27, 29, 47, 58–60). Although each of the potentiated Hsp104 variants was isolated from a screen against a single disease substrate, the majority of the variants isolated thus far rescue the toxicity of TDP-43, FUS, and α-synuclein (27). Certain variants also suppress dopaminergic neurodegeneration in a *Caenorhabditis elegans* model of Parkinson's disease (27). They also reverse FUS aggregation in fibroblasts while restoring proper localization of FUS-associated RNA (30). Surprisingly, although these variants rescue diverse substrates harboring PrLDs, they do not suppress the toxicity and aggregation of EWSR1, which has a domain architecture strikingly similar to that of FUS (29).

Here, we explored the effects of FUS-CHOP and EWS-FLI overexpression in yeast and found that they are toxic and aggregate in patterns resembling those in sarcoma patients. We further demonstrate that FUS-CHOP undergoes aberrant phase separation, adopting a gel- or solid-like state. We also demonstrate that just as the potentiated Hsp104 variants counter the toxicity of FUS, they can also suppress the toxicity of the FUS-CHOP and EWS-FLI translocations. We therefore propose that these yeast model systems might be useful platforms for studying the underpinnings of sarcoma as well as for screening for modifiers of these disorders. Moreover, we suggest that engineered protein disaggregases might be employed to combat aberrant phenotypes driven by prion-like fusion proteins involved in sarcoma and other cancers.

Results

FUS-CHOP is toxic and aggregates when expressed in yeast

FUS is a nuclear RNA-binding protein with a PrLD that forms cytoplasmic aggregates in the degenerating neurons of FUS-ALS and FTD patients (10). FUS forms toxic cytoplasmic aggregates in yeast just as it does in the degenerating neurons of ALS/FTD patients (7, 21). Therefore, we established a similar model for studying the expression of the FUS-CHOP translocation, which is implicated in liposarcoma (Fig. 1*A*) (1).

To assess FUS-CHOP toxicity and probe the domain requirements that might drive this toxicity, we expressed FUS-CHOP and several related constructs in yeast (Fig. 1*A*). We used the 413GAL plasmid to drive galactose-inducible expression of these genes, and we expressed 413GAL (empty vector), 413GAL-FUS, 413GAL-FUS-CHOP, 413GAL-FUS(1–266), and 413GAL-CHOP. FUS-CHOP overexpression was highly toxic and slightly more toxic than full-length FUS (Fig. 1*B*). The FUS(1–266) truncation was not toxic (Fig. 1*B*), corroborating studies demonstrating that the PrLD, RNA-recognition motif (RRM), and first arginine/glycine-rich (RGG) domain are required for FUS toxicity in yeast (7, 21). Furthermore, overexpression of CHOP alone is only very slightly toxic (Fig. 1*B*). These results demonstrate that both CHOP and the PrLD of FUS are required to elicit severe FUS-CHOP toxicity. We confirmed that each of the proteins was expressed by using anti-FUS and anti-CHOP antibodies (Fig. 1*C*). Each of the proteins was expressed, and FUS(1–266) was expressed at a lower level.

Using fluorescence microscopy, we established that FUS-CHOP-GFP forms nuclear foci in yeast (Fig. 1*D*) just as it does in myxoid liposarcoma cells (62, 63). FUS(1–266)-GFP displays more diffuse fluorescence than FUS-CHOP-GFP with some nuclear foci (Fig. 1*D*). Furthermore, CHOP-GFP accumulates diffusely in the nucleus, correlating with its role as a transcription factor. To confirm the fusion to GFP did not substantially alter the toxicity of these proteins, we repeated spotting assays for the GFP-tagged constructs, and results were similar to those for the untagged constructs (Fig. 1, *B* and *E*). Thus, the nonaggregating CHOP is minimally toxic, and aggregation of FUS(1–266) is not toxic (7). Because FUS(1–266) does not bind nucleic acid (64), these findings suggest that aggregation of the PrLD alone is not sufficient for toxicity. Rather, these findings suggest that constructs must aggregate *and* be capable of engaging nucleic acid to confer toxicity as with FUS-CHOP and full-length FUS (7, 65, 66). Likewise, TDP-43 must aggregate *and* be able to engage RNA to elicit toxicity in yeast and other model systems (19, 20, 67–69).

In summary, FUS-CHOP aggregates in the nucleus and is toxic in yeast, recapitulating cancer cell phenotypes observed in liposarcoma patients (62, 63). Our results suggest that yeast is an excellent model system for studying FUS-CHOP aggregation and toxicity and that this yeast model might be a suitable platform for unearthing small-molecule or genetic modulators of FUS-CHOP aggregation and toxicity.

EWS-FLI is toxic and aggregates when expressed in yeast

Like FUS, EWSR1 is an RNA-binding protein with a PrLD, and its aggregation is implicated in a subset of ALS and FTD patients (8, 70, 71). Thus, we also assessed the toxicity of EWS-FLI in yeast and performed similar domain-mapping experiments (Fig. 2*A*). Here, we expressed EWS-FLI1 and EWS-FLI3 in yeast from the galactose-inducible 413GAL plasmid along with controls 413GAL (empty vector), 413GAL-EWSR1, 423GAL-EWSR1, 413GAL-EWS(1–264), 413GAL-EWS(1–

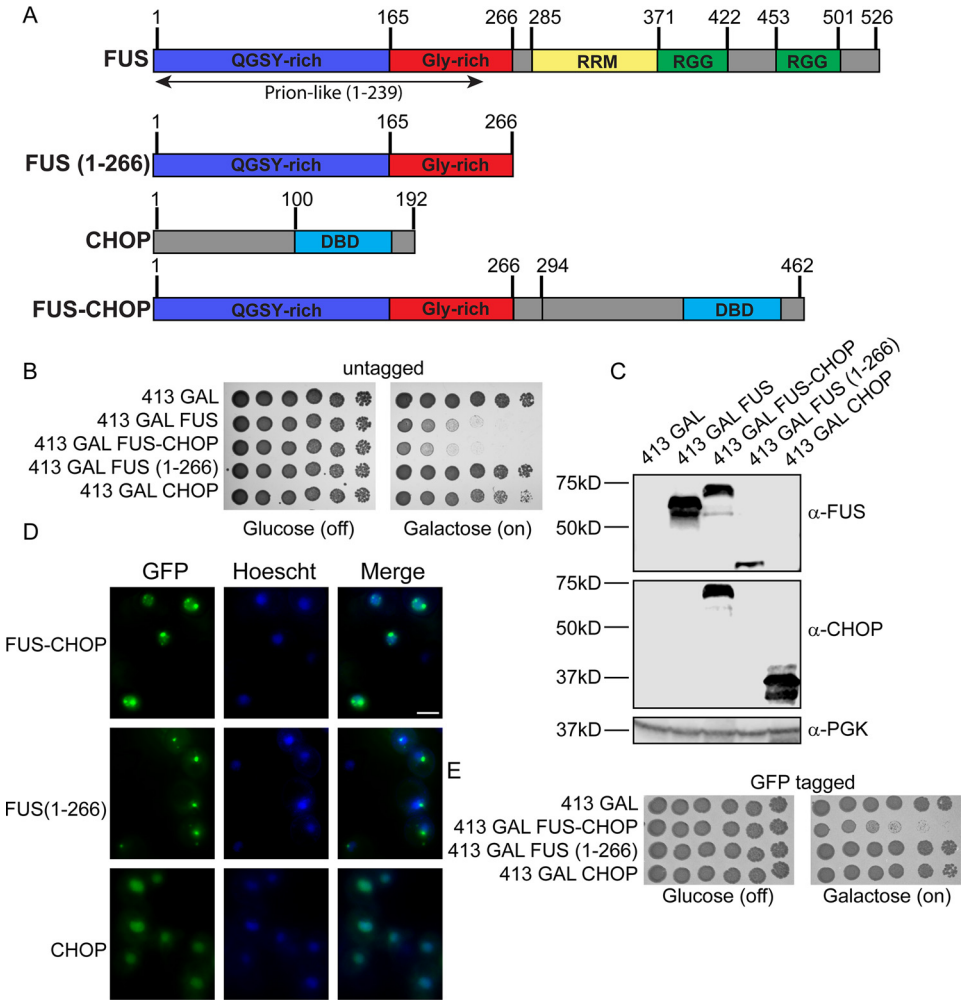

Figure 1. FUS-CHOP is toxic and forms nuclear foci in yeast. *A*, domain architecture of FUS, the FUS-CHOP fusion, and the truncations tested in this work. *DBD*, DNA-binding domain. *B*, W303Δ*hsp104* yeast was transformed with galactose-inducible FUS, FUS-CHOP, or the indicated truncation. The strains were serially diluted 5-fold and spotted on glucose (off) or galactose (on) media. *C*, strains from *B* were induced for 5 h, lysed, and immunoblotted. PGK1 serves as a loading control. *D*, fluorescence microscopy of cells expressing FUS-CHOP-GFP or the truncations stained with Hoechst dye to visualize nuclei (*blue*). *Scale bar*, 5 μm. *E*, strains from *D* were spotted on glucose and galactose media as in *B*.

347), and 413GAL-FLI (Fig. 2*B*). EWS-FLI1 and EWS-FLI3 overexpression was highly toxic and far more toxic than full-length EWSR1 when expressed at similar levels (Fig. 2, *B* and *C*). We also expressed EWSR1 from a 2μ plasmid to increase EWSR1 expression. Even at these higher expression levels (Fig. 2*C*), the EWS-FLI constructs are more toxic than EWSR1 (Fig. 2*B*). Expression of neither EWS(1–264) nor EWS(1–347) was toxic, and expression of FLI was only slightly toxic. Thus, the fusion of a portion of the EWSR1 PrLD to FLI confers a synergistic enhancement of toxicity in yeast. We confirmed that each of these proteins was expressed by using anti-EWS and anti-FLI antibodies (Fig. 2*C*). Although each of the proteins was expressed, detection of the EWS(1–264) truncation was weaker (Fig. 2*C*).

Next, we assessed the aggregation of these constructs in yeast. We first constructed GFP-tagged versions of the strains and confirmed that their toxicity was similar to that of the untagged constructs (Fig. 2, *B* and *D*). We next confirmed that EWS-FLI1-GFP and EWS-FLI3-GFP aggregate in yeast and found that these foci accumulate in the nucleus (Fig. 2*E*). As with FUS(1–266), expression of EWS(1–264) or EWS(1–347) yielded cells with more diffuse fluorescence than EWS-FLI and some nuclear foci, although again fewer than for the EWS-FLI constructs (Fig. 2*E*). Also, as with FUS-CHOP, these constructs consisting primarily of the EWSR1 PrLD yielded larger foci than for the full-length fusion (Fig. 2*E*). Finally, consistent with its role as a transcription factor, localization of FLI alone was restricted primarily to diffuse staining inside the nucleus (Fig. 2*E*). These data suggest that, as with FUS-CHOP, the PrLD of EWSR1 must be appended to a nucleic acid–binding domain to connect aggregation and toxicity. Thus, FLI does not aggregate and is not toxic, and the PrLD portions of EWSR1 aggregate but are not toxic. By contrast, appending portions of the EWSR1 PrLD to either an RRM plus RGG domains as in EWSR1 or to a DNA-binding domain as in EWS-FLI yields proteins that aggregate and are toxic.

In summary, like FUS-CHOP, EWS-FLI1 and EWS-FLI3 aggregate and are toxic in yeast, recapitulating cellular phenotypes found in Ewing's sarcoma patients (1, 2). Our results demonstrate that yeast is an excellent model system for studying FUS-CHOP and EWS-FLI aggregation and toxicity and that these models could be excellent platforms for discovering

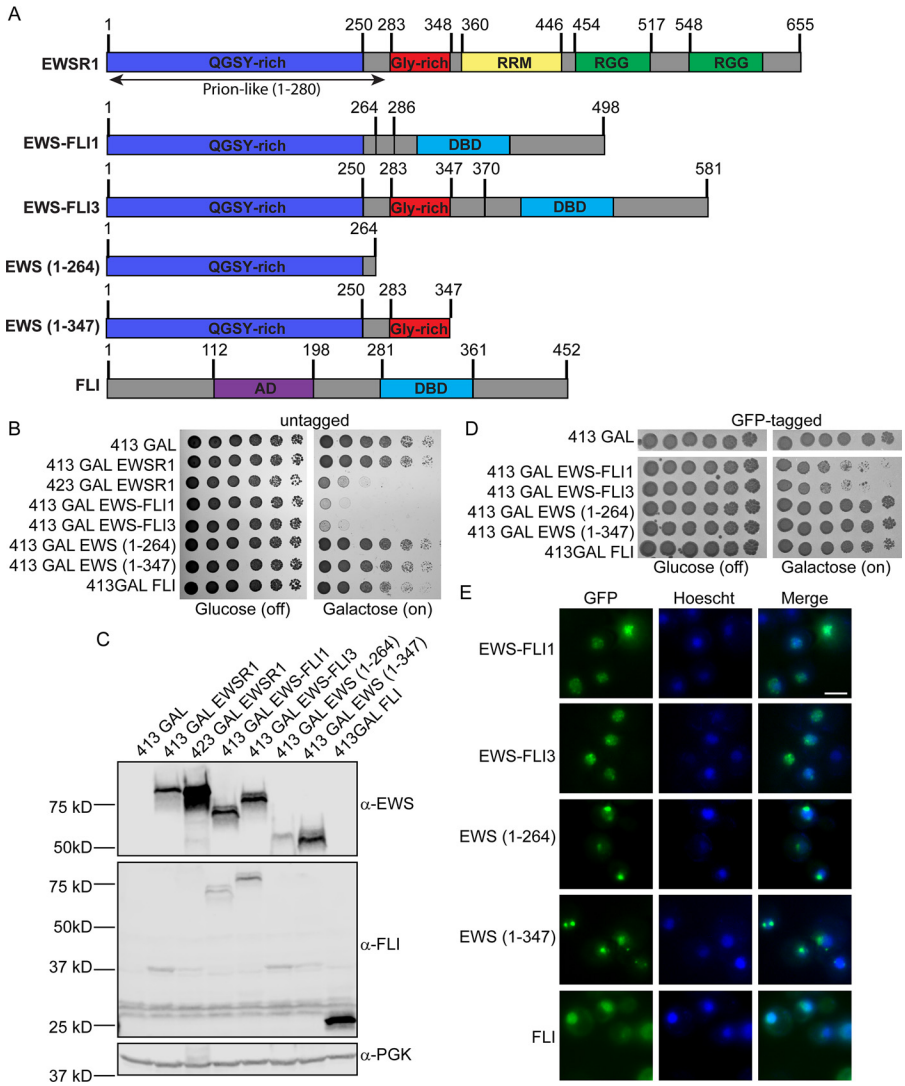

Figure 2. EWS-FLI is toxic and forms nuclear foci in yeast. *A*, domain architecture of EWSR1, EWS-FLI1, EWS-FLI3, and the corresponding truncations. *DBD*, DNA-binding domain; *AD*, activation domain. *B*, W303Δ*hsp104* yeast was transformed with galactose-inducible EWSR1, EWS-FLI1, EWS-FLI3, or the indicated truncation. The strains were serially diluted 5-fold and spotted on glucose (off) or galactose (on) media. *C*, strains from *B* were induced for 5 h, lysed, and immunoblotted. PGK1 serves as a loading control. *D*, spotting of the GFP-tagged constructs was performed as in *B*. *E*, fluorescence microscopy of cells expressing EWS-FLI1-GFP and EWS-FLI3-GFP and the truncations stained with Hoechst dye to visualize nuclei (*blue*). *Scale bar*, 5 μm.

small-molecule or genetic modifiers of the toxicity of these translocations.

FUS-CHOP protein is immobile within nuclear inclusions

It has been shown that the translocated PrLD of EWSR1 can elicit phase separation events that can disrupt transcriptional programs and lead to cancer (2). We assessed whether these same aberrant phase transitions applied to our yeast models and more broadly to FUS-CHOP. Using super-resolution imaging, we first visualized cells expressing FUS-CHOP-GFP, EWS-FLI1-GFP, or EWS-FLI3-GFP. Cells expressing FUS-CHOP-GFP were characterized by foci ~600 nm in diameter, whereas those for EWS-FLI measured less than 300 nm in diameter (Fig. 3*A*). Furthermore, the EWS-FLI foci were highly dynamic, moving rapidly throughout the nucleus. Although the FUS-CHOP inclusions also were prone to movement, this movement was slower than for EWS-FLI. As a result, we were only able to characterize the material properties of the FUS-CHOP inclusions using fluorescence recovery after photobleaching (FRAP). We employed FRAP to determine whether these inclusions displayed internal rearrangements characteristic of a liquid or a solid. Here, we photobleached a small region of the nuclear foci and tracked the recovery of fluorescence intensity within bleached and unbleached regions of interest (ROIs) by confocal microscopy (Fig. 3*B*). On following the inclusions for 90 s, we noted minimal recovery of fluorescence. Materials in the liquid state would be expected to adopt a spherical shape (72). However, the FUS-CHOP inclusions do not appear to be spherical, suggesting that FUS-CHOP adopts a gel- or solid-like state in yeast (Fig. 3*B*). For comparison, we also bleached cells expressing GFP with no fused protein. Recovery of FUS-CHOP-GFP reached only ~40% of the prebleached fluorescence intensity at most, whereas recovery of GFP exceeded 60% and was more rapid (Fig. 3*C*). Thus, we conclude that FUS-CHOP phase separates to a gel- or solid-like state.

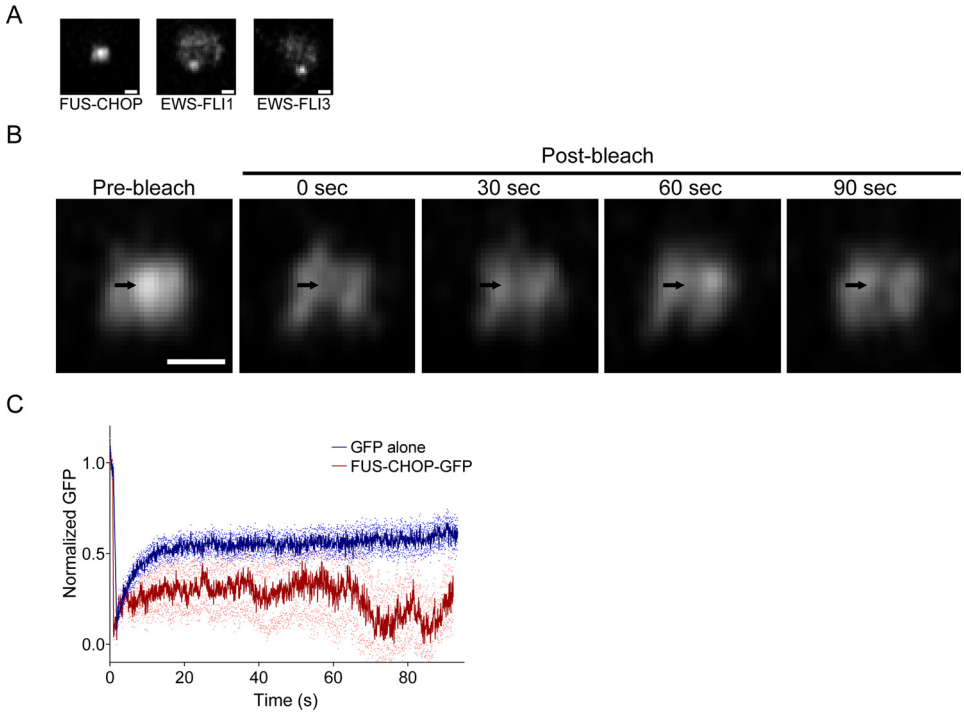

Figure 3. FUS-CHOP inclusions display gel- or solid-like properties. *A*, FUS-CHOP, EWS-FLI1, and EWS-FLI3 form nuclear foci in yeast, and FUS-CHOP foci were generally substantially larger than EWS-FLI foci. *B*, FRAP of FUS-CHOP-GFP shows that the nuclear foci are immobile and do not recover after 90 s. Also, the inclusions do not appear spherical, consistent with more gel- or solid-like properties. *Arrows* indicate the ROI that was photobleached. *C*, FRAP experiments were performed for FUS-CHOP-GFP and a diffuse GFP control. FUS-CHOP shows a slower rate of return than GFP. *Scale bars* in *A* and *B* are 500 nm. Curves in *C* show data points (*dark blue* and *red*) ± S.E. (*light blue* and *red*), $n \geq 10$ cells per condition.

Potentiated Hsp104 variants suppress FUS-CHOP toxicity and aggregation

We have previously demonstrated that engineered variants of the yeast AAA+ protein Hsp104 can suppress the aggregation and toxicity of FUS, TDP-43, and α-synuclein (27, 29, 58). Hsp104 is a protein disaggregase that translocates these substrates through its central pore and, through cycles of ATP hydrolysis, dissolves these kinetically trapped aggregates such that solubilized proteins can then refold to the native state (39, 52, 53, 73, 74). We hypothesize that, as for EWS-FLI (2), the PrLD of FUS-CHOP drives FUS-CHOP aggregation in addition to altering its transcriptional program (62, 63). Thus, development of a FUS-CHOP disaggregase might be a useful agent to counter aberrantly functioning FUS-CHOP.

We were curious whether the same Hsp104 variants that can dissolve FUS aggregates might also rescue FUS-CHOP toxicity, considering that the PrLD of FUS is conserved in the FUS-CHOP translocation (1, 27, 29). Hsp104 harbors a nuclear localization sequence and localizes to the cytoplasm and nucleus in yeast (75). Thus, Hsp104 could antagonize formation of nuclear FUS-CHOP aggregates. We coexpressed FUS-CHOP with Hsp104 and a series of potentiated variants, $Hsp104^{A503V}$, $Hsp104^{A503S}$, $Hsp104^{A503G}$, $Hsp104^{V426L}$, $Hsp104^{A437W}$, $Hsp104^{Y507C}$, $Hsp104^{N539K}$, and $Hsp104^{DPLF\text{-}A503V}$ (27). Hsp104 is inactive against FUS in yeast, and we found that Hsp104 is similarly inactive against FUS-CHOP (Fig. 4*A*). However, each of the potentiated Hsp104 variants tested potently suppressed FUS-CHOP toxicity, restoring growth to nearly the levels of vector alone (Fig. 4*A*, *top lane*, *413GAL + 416GAL*). We assessed expression levels by immunoblotting and confirmed that this toxicity suppression is not due to decreased FUS-CHOP expression (Fig. 4*B*). As we have seen in other studies (27, 29, 58), the Hsp104 variants are expressed at lower levels than Hsp104, suggesting that they are more active at lower concentrations.

We next assessed the effects of the potentiated Hsp104 variants on the FUS-CHOP nuclear foci. Here, we coexpressed FUS-CHOP-GFP with Hsp104 and two of the potentiated variants, $Hsp104^{A503V}$ and $Hsp104^{A503S}$. Although Hsp104 has no apparent effect on the FUS-CHOP-GFP foci, cells expressing either $Hsp104^{A503V}$ or $Hsp104^{A503S}$ show a reduced number and size of nuclear foci (Fig. 4, *C* and *D*). We confirmed that the Hsp104 variants only subtly decrease expression levels of FUS-CHOP-GFP (Fig. 4*E*). Because we still observed some foci, we tested the rescue of the potentiated variants against FUS-CHOP-GFP (Fig. 4*F*). We found that FUS-CHOP-GFP is less toxic than untagged FUS-CHOP, and so the rescue of toxicity is more modest than for the untagged constructs. Here, $Hsp104^{A503S}$ was more effective in rescuing toxicity than $Hsp104^{A503V}$ (Fig. 4*F*). Collectively, these findings establish that enhanced Hsp104 variants antagonize FUS-CHOP toxicity and phase separation.

Potentiated Hsp104 variants suppress EWS-FLI toxicity and aggregation

We have previously shown that the substrate repertoire of the potentiated Hsp104 variants is broad (27, 29). Thus, we hypothesized that, given the similar domain architecture of EWSR1 and FUS, Hsp104 variants that disaggregate FUS would also disaggregate EWSR1. Surprisingly, variants active against

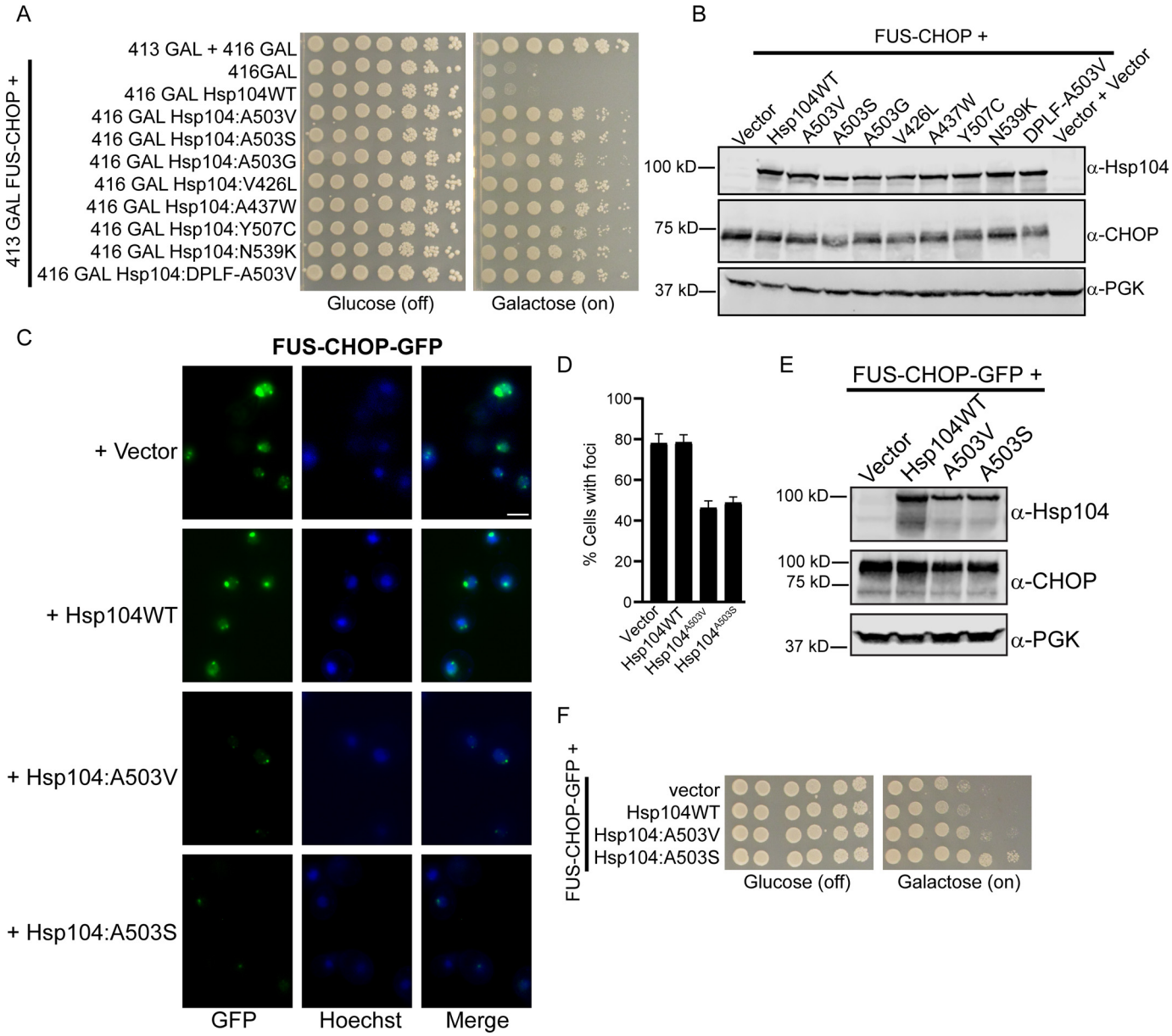

Figure 4. Potentiated Hsp104 variants suppress FUS-CHOP toxicity and aggregation. *A*, W303Δ*hsp104* yeast was sequentially transformed with FUS-CHOP and Hsp104 or the indicated variants. The strains were serially diluted 5-fold and spotted on glucose (off) or galactose (on) media. *B*, strains from *A* were induced for 5 h, lysed, and immunoblotted. *C*, W303Δ*hsp104* yeast was sequentially transformed with FUS-CHOP-GFP and Hsp104 or the indicated variants. The strains were induced for 5 h, stained with Hoechst dye, and imaged. Representative images are shown. *Scale bar*, 5 μm. *D*, quantification of microscopy experiments shown in *C*. *Error bars* represent S.E.M. *E*, strains from *C* were induced for 5 h, lysed, and immunoblotted. *F*, strains from *C* were serially diluted 5-fold and spotted on glucose and galactose media.

FUS do not rescue EWSR1 toxicity or aggregation, and some variants even enhance EWSR1 toxicity (29). Therefore, we were curious to test whether these same variants might rescue EWS-FLI toxicity. We coexpressed EWS-FLI1 and EWS-FLI3 with Hsp104 and the same series of potentiated variants tested against FUS-CHOP. Hsp104 does not suppress EWSR1 toxicity in yeast, and we found that Hsp104 does not suppress EWS-FLI1 or EWS-FLI3 toxicity either (Fig. 5, *A* and *C*). We found that, unlike with FUS-CHOP, only certain Hsp104 variants rescue EWS-FLI toxicity: Hsp104^{A503S}, Hsp104^{V426L}, Hsp104^{A437W}, Hsp104 ^{N539K}, and Hsp104$^{DPLF-A503V}$ robustly rescue EWS-FLI1 toxicity. By contrast, Hsp104^{A503V} confers a more modest rescue of EWS-FLI1 toxicity. We confirmed that this rescue was not simply due to decreased EWS-FLI1 expression levels (Fig. 5*B*). Hsp104^{A503S}, Hsp104^{A503G}, Hsp104^{N539K}, and Hsp104$^{DPLF-A503V}$ confer a strong rescue of EWS-FLI3 toxicity, whereas Hsp104^{V426L} and Hsp104^{A437W} confer a more modest rescue (Fig. 5*C*). As with EWS-FLI1, the potentiated variants rescue EWS-FLI3 toxicity without substantially modifying EWS-FLI3 expression levels (Fig. 5*D*). Like we have seen with FUS-CHOP, the Hsp104 variants are expressed at lower levels than Hsp104, indicating that they are active even when expressed at lower concentrations. Although Hsp104^{A503S} and Hsp104^{V426L} suppress the toxicity of both EWS-FLI1 and EWS-FLI3, these same variants do not rescue EWSR1 toxicity (29). These results suggest that translocation of the EWSR1 PrLD to

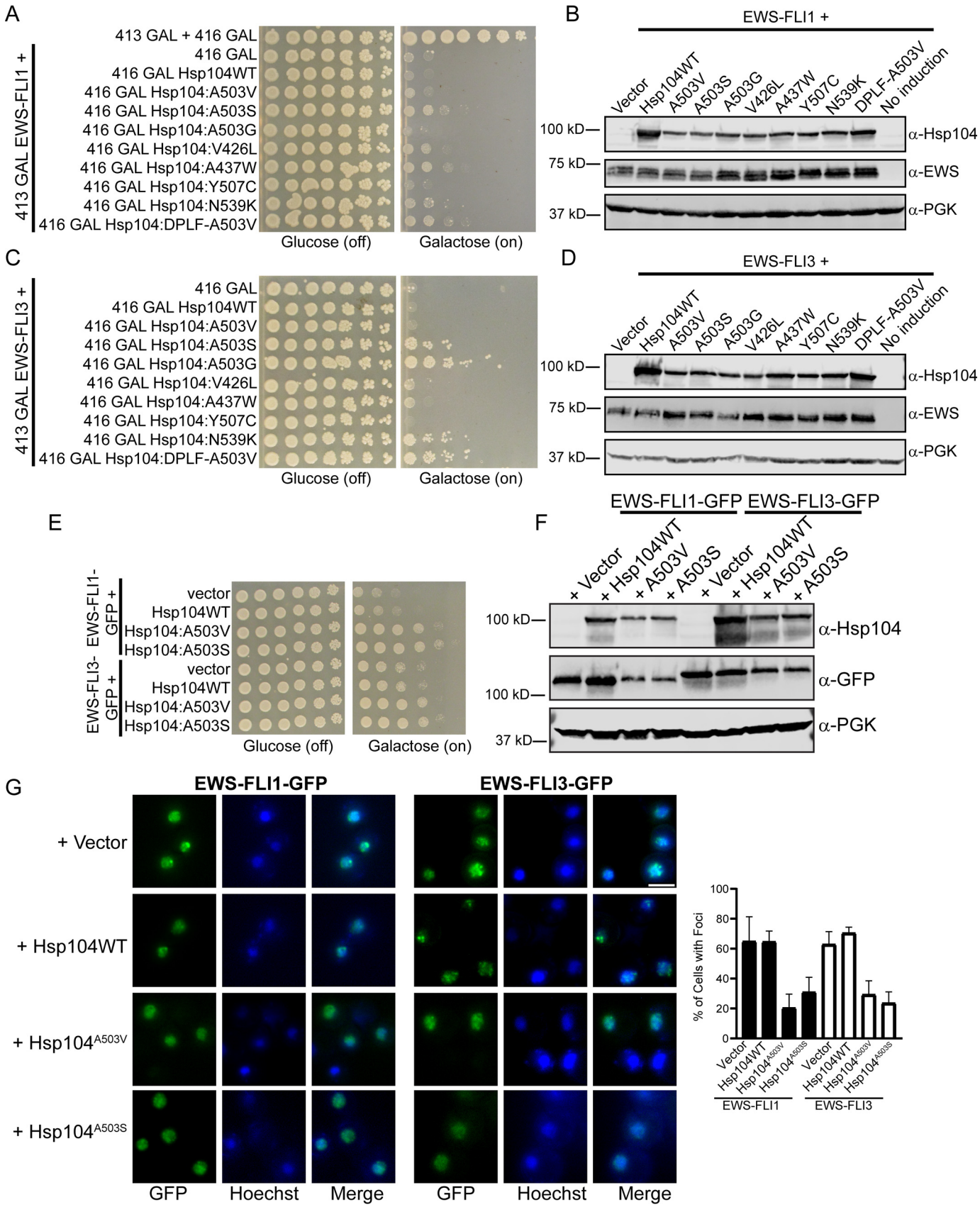
A
413 GAL EWS-FLI1 +
413 GAL + 416 GAL
416 GAL
416 GAL Hsp104WT
416 GAL Hsp104:A503V
416 GAL Hsp104:A503S
416 GAL Hsp104:A503G
416 GAL Hsp104:V426L
416 GAL Hsp104:A437W
416 GAL Hsp104:Y507C
416 GAL Hsp104:N539K
416 GAL Hsp104:DPLF-A503V
Glucose (off)
Galactose (on)
B
EWS-FLI1 +
Vector
Hsp104WT
A503V
A503S
A503G
V426L
A437W
Y507C
N539K
DPLF-A503V
No induction
100 kD
75 kD
37 kD
α-Hsp104
α-EWS
α-PGK
C
413 GAL EWS-FLI3 +
416 GAL
416 GAL Hsp104WT
416 GAL Hsp104:A503V
416 GAL Hsp104:A503S
416 GAL Hsp104:A503G
416 GAL Hsp104:V426L
416 GAL Hsp104:A437W
416 GAL Hsp104:Y507C
416 GAL Hsp104:N539K
416 GAL Hsp104:DPLF-A503V
Glucose (off)
Galactose (on)
D
EWS-FLI3 +
Vector
Hsp104WT
A503V
A503S
A503G
V426L
A437W
Y507C
N539K
DPLF-A503V
No induction
100 kD
75 kD
37 kD
α-Hsp104
α-EWS
α-PGK
E
EWS-FLI1-GFP +
EWS-FLI3-GFP +
vector
Hsp104WT
Hsp104:A503V
Hsp104:A503S
Glucose (off)
Galactose (on)
F
EWS-FLI1-GFP
EWS-FLI3-GFP
+ Vector
+ Hsp104WT
+ A503V
+ A503S
100 kD
100 kD
37 kD
α-Hsp104
α-GFP
α-PGK
G
EWS-FLI1-GFP
EWS-FLI3-GFP
+ Vector
+ Hsp104WT
+ Hsp104A503V
+ Hsp104A503S
GFP
Hoechst
Merge
% of Cells with Foci
Vector
Hsp104WT
Hsp104A503V
Hsp104A503S
EWS-FLI1
EWS-FLI3

FLI yields a protein with physical properties distinct from EWSR1, allowing for detoxifying remodeling by the potentiated Hsp104 variants.

We next assessed the effects of the potentiated Hsp104 variants on the EWS-FLI nuclear foci. Here, we coexpressed EWS-FLI1-GFP or EWS-FLI3-GFP with Hsp104 or two of the potentiated variants that conferred a mild ($Hsp104^{A503V}$) and more moderate ($Hsp104^{A503S}$) rescue of toxicity. We first retested these variants against the EWS-FLI-GFP fusions to confirm they still rescue toxicity (Fig. 5*E*). EWS-FLI1-GFP and EWS-FLI3-GFP are both less toxic than their untagged versions, and so the potentiated Hsp104 variants rescue this toxicity more robustly. We then confirmed expression via immunoblotting and found that the Hsp104 variants decrease the expression of EWS-FLI-GFP more than they do for EWS-FLI (Fig. 5*B*, *D* and *F*). Using fluorescence microscopy, we found that, although Hsp104 has no effect on the EWS-FLI foci, cells expressing either $Hsp104^{A503V}$ or $Hsp104^{A503S}$ reduced nuclear foci (Fig. 5*G*). Collectively, our findings suggest that enhanced Hsp104 variants antagonize EWS-FLI toxicity and phase separation.

Discussion

Here, we have established yeast models to investigate the misfolding of FUS-CHOP and EWS-FLI translocations that underpin sarcoma. We found that fusion of FUS and EWS to CHOP and FLI, respectively, drives a synergistic enhancement in toxicity of the resulting fusions. As in sarcoma patients, FUS-CHOP and EWS-FLI expression in yeast leads to the formation of multiple nuclear foci. We found that FUS-CHOP foci display properties characteristic of a gel or solid rather than a liquid. Aggregation *and* nucleic acid– binding capability were important for toxicity as CHOP or FLI did not aggregate and were not toxic, and portions of the PrLDs of FUS or EWSR1 (which do not bind RNA) aggregated but were not toxic. In this regard, FUS-CHOP and EWS-FLI toxicity resembles FUS and TDP-43 toxicity in yeast where nucleic acid binding couples aggregation to toxicity (7, 19–21).

We also have demonstrated that potentiated Hsp104 variants that suppress FUS toxicity also robustly suppress the toxicity of FUS-CHOP and EWS-FLI. These Hsp104 variants also decrease the accumulation of nuclear foci of FUS-CHOP and EWS-FLI. It is important to note that, although these Hsp104 variants cannot counter the toxicity of EWSR1 (29), they do counter the toxicity of EWS-FLI. Thus, the EWS-FLI translocation yields a protein with a distinct structure, which enables the Hsp104 variants to remodel EWS-FLI even though they do not remodel EWSR1.

Recently, it has been demonstrated that the PrLD of EWS-FLI drives phase separation and that this phase separation activates the transcriptional events of Ewing's sarcoma (2, 12). Hsp104 has been shown to regulate phase transitions in yeast (41, 48, 76). Thus, it will be interesting to determine whether the potentiated variants can also antagonize aberrant phase transitions of EWS-FLI or FUS-CHOP in sarcoma patient cells.

It has been demonstrated that many complex diseases can be modeled in yeast (7, 20–22, 77–79), and we now demonstrate that the aberrant phase transitions of FUS-CHOP and EWS-FLI that underlie sarcoma can also be modeled in yeast. We anticipate that these new model systems will serve as robust platforms to enable rapid genome-wide and small-molecule screens in yeast to identify additional modifiers of FUS-CHOP and EWS-FLI aggregation and toxicity.

We have demonstrated that Hsp104, which regulates yeast prions (80), can be potentiated to counter the toxicity of FUS, TDP-43, α-synuclein, and now FUS-CHOP and EWS-FLI as well (27, 29). It is intriguing that the specificity Hsp104 has for yeast prions carries over to substrates that form amyloid or prion-like structures in humans even though yeast Hsp104 has not encountered these exact substrates throughout evolution. In the future, it will be interesting to assess whether these enhanced disaggregases can also block the aberrant transcriptional programs driven by FUS-CHOP and EWS-FLI in sarcoma.

Experimental procedures

All yeast were WT W303a Δ*hsp104* (*MATa, can1–100, his3–11,15, leu2-3,112, trp1-1, ura3-1, ade2-1*) (81). Yeast were grown in rich medium (yeast extract, peptone, dextrose (YPD)) or in synthetic media lacking the appropriate amino acids. Media were supplemented with 2% glucose, raffinose, or galactose. Vectors encoding FUS-CHOP and EWS-FLI were obtained from Addgene and Jeffrey Toretsky, respectively. The FUS and EWSR1 plasmids were described previously (27, 29). Vectors were cloned from these plasmids into pDONR 221 and then transferred to pAG413GAL via Gateway cloning. pAG416GAL-Hsp104 and the potentiated variants were generated previously (27). All truncated constructs were generated using QuikChange site-directed mutagenesis (Agilent), and all constructs were confirmed by DNA sequencing.

Yeast were transformed according to standard protocols using PEG and lithium acetate (82). Yeast strains were constructed by first transforming the appropriate pAG413GAL plasmid. Plates were then scraped, and cultures were inoculated and subsequently transformed with the pAG416GAL-Hsp104 plasmids. For the spotting assays, yeast were grown to saturation overnight in raffinose-supplemented dropout media at 30 °C. Cultures were serially diluted 5-fold and spotted in duplicate onto synthetic dropout media containing glucose or galactose. Plates were analyzed after growth for 2–3 days at 30 °C.

For immunoblotting, yeast were grown overnight to saturation in raffinose. They were then diluted to an $A_{600\ nm}$ of 0.3 in galactose-containing media and induced for 5 h. Cultures were normalized to an $A_{600\ nm}$ of 0.6, 3 ml of cells were harvested and treated in 0.1 M NaOH for 5 min at room temperature, and cell

Figure 5. Potentiated Hsp104 variants suppress EWS-FLI1 and EWS-FLI3 toxicity and aggregation. *A*, W303Δ*hsp104* yeast was sequentially transformed with EWS-FLI1 and Hsp104 or the indicated variants. The strains were serially diluted 5-fold and spotted on glucose (off) or galactose (on) media. *B*, strains from *A* were induced for 5 h, lysed, and immunoblotted. *C*, experiments were performed as in *A* but using EWS-FLI3. *D*, strains from *C* were induced for 5 h, lysed, and immunoblotted. *E*, W303Δ*hsp104* yeast was sequentially transformed with EWS-FLI1-GFP or EWS-FLI3-GFP and Hsp104 or the indicated variants. *F*, strains from *E* were induced for 5 h, lysed, and immunoblotted. *G*, *left*, strains from *E* were induced for 5 h, stained with Hoechst dye, and imaged. *Scale bar*, 5 μm. *Right*, quantification of microscopy. *Error bars* represent S.E.M.

pellets were then resuspended into 1× SDS sample buffer and boiled for 10 min. Lysates were cleared by centrifugation at 14,000 rpm for 2 min, then separated by SDS-PAGE (4–20% gradient; Bio-Rad), and transferred to a polyvinylidene difluoride membrane. Membranes were blocked in LI-COR Biosciences Odyssey PBS blocking buffer for 2 h at room temperature. Primary antibody incubations were performed at 4 °C overnight. Antibodies used included anti-FUS polyclonal (Bethyl Laboratories), anti-Hsp104 polyclonal (Enzo Life Sciences), anti-3-phosphoglycerate kinase (PGK) monoclonal (Invitrogen), anti-CHOP (Abcam), anti-EWS (Santa Cruz Biotechnology), and anti-FLI (Abcam). Blots were processed using a LI-COR Biosciences Odyssey Fc imaging system.

For fluorescence microscopy, FUS-CHOP, EWS-FLI1, and EWS-FLI3 were imaged by appending a C-terminal GFP tag using Gateway cloning into pAG303GAL-ccdB-GFP. The pAG303GAL-FUS-CHOP-GFP, pAG303GAL-EWS-FLI1-GFP, and pAG303GAL-EWS-FLI3-GFP were then linearized and transformed as described above. Single colonies were selected, and yeast were grown and processed for microscopy as for immunoblotting. To assess the effects of Hsp104 on FUS-CHOP and EWS-FLI nuclear foci, these strains were then sequentially transformed with pAG416GAL, pAG416GAL-Hsp104, or variants of Hsp104. For imaging the truncation variants, the pAG413GAL-ccdB-GFP plasmid was used in place of pAG303GAL-ccdB-GFP. After 5-h induction at 30 °C, cultures were harvested and processed for microscopy. All imaging was performed using live cells treated with Hoechst dye. Images were collected at 100× magnification using a Leica DM IRBE microscope or a Nikon Eclipse Te2000-E microscope and processed using ImageJ software. All experiments were repeated at least three times, and representative images are shown.

For FRAP experiments, yeast were harvested after 5-h induction at 30 °C. Yeast were immobilized on slides using a 4% agarose pad supplemented with media and sealed with nail polish. Images were acquired using a Zeiss LSM 880 confocal microscope with Airyscan. For FUS-CHOP-GFP strains, a 1 × 1-pixel ROI was drawn in the center of the focus. For diffuse GFP, an 8 × 8-pixel circular ROI was drawn. ROIs were photobleached using a 488 nm laser at 60% power for 15 iterations of 16 μs/pixel and imaged for fluorescence recovery for 90 s at 0.0618 s/frame after bleaching using the Airyscan detector. Images were deconvolved with a 2.7 Airyscan parameter.

Image analysis was performed in Fiji. The GFP integrated densities of the bleached area, background, and a reference cell were calculated. Individual curves were background-subtracted and corrected for bleaching caused by imaging. Individual curves were normalized to the average of pre-bleach integrated densities and the postbleach minimum. Individual curves were then averaged to produce a single FRAP curve.

Author contributions—J. J. R., M. L. S., K. H., and M. E. J. investigation; J. S. and M. E. J. conceptualization; J. S. and M. E. J. formal analysis; J. S. and M. E. J. supervision; J. S. and M. E. J. funding acquisition; J. S. and M. E. J. writing-original draft; J. S. and M. E. J. writing-review and editing; M. E. J. resources.

Acknowledgments—We thank Peter Bayguinov and James Fitzpatrick of the Washington University Center for Cellular Imaging for assistance with microscopy. We thank Zach March, Korrie Mack, and Bede Portz for review of the manuscript and Jeffrey Toretsky for providing plasmids. Confocal data were generated on a Zeiss LSM 880 Airyscan confocal microscope, which was purchased with support from the Office of Research Infrastructure Programs (ORIP), a part of the National Institutes of Health Office of the Director, under Grant OD021629.

References

1. Tan, A. Y., and Manley, J. L. (2009) The TET family of proteins: functions and roles in disease. *J. Mol. Cell Biol.* **1,** 82–92 CrossRef Medline
2. Boulay, G., Sandoval, G. J., Riggi, N., Iyer, S., Buisson, R., Naigles, B., Awad, M. E., Rengarajan, S., Volorio, A., McBride, M. J., Broye, L. C., Zou, L., Stamenkovic, I., Kadoch, C., and Rivera, M. N. (2017) Cancer-specific retargeting of BAF complexes by a prion-like domain. *Cell* **171,** 163–178.e19 CrossRef Medline
3. Cushman, M., Johnson, B. S., King, O. D., Gitler, A. D., and Shorter, J. (2010) Prion-like disorders: blurring the divide between transmissibility and infectivity. *J. Cell Sci.* **123,** 1191–1201 CrossRef Medline
4. King, O. D., Gitler, A. D., and Shorter, J. (2012) The tip of the iceberg: RNA-binding proteins with prion-like domains in neurodegenerative disease. *Brain Res.* **1462,** 61–80 CrossRef Medline
5. March, Z. M., King, O. D., and Shorter, J. (2016) Prion-like domains as epigenetic regulators, scaffolds for subcellular organization, and drivers of neurodegenerative disease. *Brain Res.* **1647,** 9–18 CrossRef Medline
6. Harrison, A. F., and Shorter, J. (2017) RNA-binding proteins with prion-like domains in health and disease. *Biochem. J.* **474,** 1417–1438 CrossRef Medline
7. Sun, Z., Diaz, Z., Fang, X., Hart, M. P., Chesi, A., Shorter, J., and Gitler, A. D. (2011) Molecular determinants and genetic modifiers of aggregation and toxicity for the ALS disease protein FUS/TLS. *PLoS Biol.* **9,** e1000614 CrossRef Medline
8. Couthouis, J., Hart, M. P., Erion, R., King, O. D., Diaz, Z., Nakaya, T., Ibrahim, F., Kim, H. J., Mojsilovic-Petrovic, J., Panossian, S., Kim, C. E., Frackelton, E. C., Solski, J. A., Williams, K. L., Clay-Falcone, D., *et al.* (2012) Evaluating the role of the FUS/TLS-related gene EWSR1 in amyotrophic lateral sclerosis. *Hum. Mol. Genet.* **21,** 2899–2911 CrossRef Medline
9. Couthouis, J., Hart, M. P., Shorter, J., DeJesus-Hernandez, M., Erion, R., Oristano, R., Liu, A. X., Ramos, D., Jethava, N., Hosangadi, D., Epstein, J., Chiang, A., Diaz, Z., Nakaya, T., Ibrahim, F., *et al.* (2011) A yeast functional screen predicts new candidate ALS disease genes. *Proc. Natl. Acad. Sci. U.S.A.* **108,** 20881–20890 CrossRef Medline
10. Robberecht, W., and Philips, T. (2013) The changing scene of amyotrophic lateral sclerosis. *Nat. Rev. Neurosci.* **14,** 248–264 CrossRef Medline
11. Taylor, J. P., Brown, R. H., Jr., and Cleveland, D. W. (2016) Decoding ALS: from genes to mechanism. *Nature* **539,** 197–206 CrossRef Medline
12. Kwon, I., Kato, M., Xiang, S., Wu, L., Theodoropoulos, P., Mirzaei, H., Han, T., Xie, S., Corden, J. L., and McKnight, S. L. (2013) Phosphorylation-regulated binding of RNA polymerase II to fibrous polymers of low-complexity domains. *Cell* **155,** 1049–1060 CrossRef Medline
13. Kato, M., Han, T. W., Xie, S., Shi, K., Du, X., Wu, L. C., Mirzaei, H., Goldsmith, E. J., Longgood, J., Pei, J., Grishin, N. V., Frantz, D. E., Schneider, J. W., Chen, S., Li, L., *et al.* (2012) Cell-free formation of RNA granules: low complexity sequence domains form dynamic fibers within hydrogels. *Cell* **149,** 753–767 CrossRef Medline
14. Shorter, J. (2017) Prion-like domains program Ewing's sarcoma. *Cell* **171,** 30–31 CrossRef Medline
15. Boeynaems, S., Alberti, S., Fawzi, N. L., Mittag, T., Polymenidou, M., Rousseau, F., Schymkowitz, J., Shorter, J., Wolozin, B., Van Den Bosch, L., Tompa, P., and Fuxreiter, M. (2018) Protein phase separation: a new phase in cell biology. *Trends Cell. Biol.* **28,** 420–435 CrossRef Medline

16. Guo, L., and Shorter, J. (2015) It's raining liquids: RNA tunes viscoelasticity and dynamics of membraneless organelles. *Mol. Cell* **60,** 189–192 CrossRef Medline
17. Chung, C. Y., Khurana, V., Auluck, P. K., Tardiff, D. F., Mazzulli, J. R., Soldner, F., Baru, V., Lou, Y., Freyzon, Y., Cho, S., Mungenast, A. E., Muffat, J., Mitalipova, M., Pluth, M. D., Jui, N. T., *et al.* (2013) Identification and rescue of alpha-synuclein toxicity in Parkinson patient-derived neurons. *Science* **342,** 983–987 CrossRef Medline
18. Cooper, A. A., Gitler, A. D., Cashikar, A., Haynes, C. M., Hill, K. J., Bhullar, B., Liu, K., Xu, K., Strathearn, K. E., Liu, F., Cao, S., Caldwell, K. A., Caldwell, G. A., Marsischky, G., Kolodner, R. D., *et al.* (2006) α-Synuclein blocks ER-Golgi traffic and Rab1 rescues neuron loss in Parkinson's models. *Science* **313,** 324–328 CrossRef Medline
19. Elden, A. C., Kim, H. J., Hart, M. P., Chen-Plotkin, A. S., Johnson, B. S., Fang, X., Armakola, M., Geser, F., Greene, R., Lu, M. M., Padmanabhan, A., Clay-Falcone, D., McCluskey, L., Elman, L., Juhr, D., *et al.* (2010) Ataxin-2 intermediate-length polyglutamine expansions are associated with increased risk for ALS. *Nature* **466,** 1069–1075 CrossRef Medline
20. Johnson, B. S., McCaffery, J. M., Lindquist, S., and Gitler, A. D. (2008) A yeast TDP-43 proteinopathy model: exploring the molecular determinants of TDP-43 aggregation and cellular toxicity. *Proc. Natl. Acad. Sci. U.S.A.* **105,** 6439–6444 CrossRef Medline
21. Ju, S., Tardiff, D. F., Han, H., Divya, K., Zhong, Q., Maquat, L. E., Bosco, D. A., Hayward, L. J., Brown, R. H., Jr., Lindquist, S., Ringe, D., and Petsko, G. A. (2011) A yeast model of FUS/TLS-dependent cytotoxicity. *PLoS Biol.* **9,** e1001052 CrossRef Medline
22. Outeiro, T. F., and Lindquist, S. (2003) Yeast cells provide insight into α-synuclein biology and pathobiology. *Science* **302,** 1772–1775 CrossRef Medline
23. Tardiff, D. F., Jui, N. T., Khurana, V., Tambe, M. A., Thompson, M. L., Chung, C. Y., Kamadurai, H. B., Kim, H. T., Lancaster, A. K., Caldwell, K. A., Caldwell, G. A., Rochet, J. C., Buchwald, S. L., and Lindquist, S. (2013) Yeast reveal a "druggable" Rsp5/Nedd4 network that ameliorates α-synuclein toxicity in neurons. *Science* **342,** 979–983 CrossRef Medline
24. Treusch, S., Hamamichi, S., Goodman, J. L., Matlack, K. E., Chung, C. Y., Baru, V., Shulman, J. M., Parrado, A., Bevis, B. J., Valastyan, J. S., Han, H., Lindhagen-Persson, M., Reiman, E. M., Evans, D. A., Bennett, D. A., *et al.* (2011) Functional links between Aβ toxicity, endocytic trafficking, and Alzheimer's disease risk factors in yeast. *Science* **334,** 1241–1245 CrossRef Medline
25. Becker, L. A., Huang, B., Bieri, G., Ma, R., Knowles, D. A., Jafar-Nejad, P., Messing, J., Kim, H. J., Soriano, A., Auburger, G., Pulst, S. M., Taylor, J. P., Rigo, F., and Gitler, A. D. (2017) Therapeutic reduction of ataxin-2 extends lifespan and reduces pathology in TDP-43 mice. *Nature* **544,** 367–371 CrossRef Medline
26. Johnson, B. S., Snead, D., Lee, J. J., McCaffery, J. M., Shorter, J., and Gitler, A. D. (2009) TDP-43 is intrinsically aggregation-prone, and amyotrophic lateral sclerosis-linked mutations accelerate aggregation and increase toxicity. *J. Biol. Chem.* **284,** 20329–20339 CrossRef Medline
27. Jackrel, M. E., DeSantis, M. E., Martinez, B. A., Castellano, L. M., Stewart, R. M., Caldwell, K. A., Caldwell, G. A., and Shorter, J. (2014) Potentiated Hsp104 variants antagonize diverse proteotoxic misfolding events. *Cell* **156,** 170–182 CrossRef Medline
28. Guo, L., Kim, H. J., Wang, H., Monaghan, J., Freyermuth, F., Sung, J. C., O'Donovan, K., Fare, C. M., Diaz, Z., Singh, N., Zhang, Z. C., Coughlin, M., Sweeny, E. A., DeSantis, M. E., Jackrel, M. E., *et al.* (2018) Nuclear-import receptors reverse aberrant phase transitions of RNA-binding proteins with prion-like domains. *Cell* **173,** 677–692.e20 CrossRef Medline
29. Jackrel, M. E., and Shorter, J. (2014) Potentiated Hsp104 variants suppress toxicity of diverse neurodegenerative disease-linked proteins. *Dis. Model. Mech.* **7,** 1175–1184 CrossRef Medline
30. Yasuda, K., Clatterbuck-Soper, S. F., Jackrel, M. E., Shorter, J., and Mili, S. (2017) FUS inclusions disrupt RNA localization by sequestering kinesin-1 and inhibiting microtubule detyrosination. *J. Cell Biol.* **216,** 1015–1034 CrossRef Medline
31. Jakobson, C. M., and Jarosz, D. F. (2018) Organizing biochemistry in space and time using prion-like self-assembly. *Curr. Opin. Syst. Biol.* **8,** 16–24 CrossRef Medline
32. Shorter, J., and Lindquist, S. (2005) Prions as adaptive conduits of memory and inheritance. *Nat. Rev. Genet.* **6,** 435–450 CrossRef Medline
33. Harvey, Z. H., Chen, Y., and Jarosz, D. F. (2018) Protein-based inheritance: epigenetics beyond the chromosome. *Mol. Cell* **69,** 195–202 CrossRef Medline
34. Halfmann, R., Alberti, S., and Lindquist, S. (2010) Prions, protein homeostasis, and phenotypic diversity. *Trends Cell Biol.* **20,** 125–133 CrossRef Medline
35. Newby, G. A., and Lindquist, S. (2013) Blessings in disguise: biological benefits of prion-like mechanisms. *Trends Cell Biol.* **23,** 251–259 CrossRef Medline
36. Chuang, E., Hori, A. M., Hesketh, C. D., and Shorter, J. (2018) Amyloid assembly and disassembly. *J. Cell Sci.* **131,** jcs189928 CrossRef Medline
37. DeSantis, M. E., and Shorter, J. (2012) Hsp104 drives "protein-only" positive selection of Sup35 prion strains encoding strong [PSI$^+$]. *Chem. Biol.* **19,** 1400–1410 CrossRef Medline
38. Glover, J. R., and Lindquist, S. (1998) Hsp104, Hsp70, and Hsp40: a novel chaperone system that rescues previously aggregated proteins. *Cell* **94,** 73–82 CrossRef Medline
39. Jackrel, M. E., and Shorter, J. (2017) Protein-remodeling factors as potential therapeutics for neurodegenerative disease. *Front. Neurosci.* **11,** 99 CrossRef Medline
40. Klaips, C. L., Hochstrasser, M. L., Langlois, C. R., and Serio, T. R. (2014) Spatial quality control bypasses cell-based limitations on proteostasis to promote prion curing. *Elife* **3,** e04288 CrossRef Medline e04288
41. Kroschwald, S., Maharana, S., Mateju, D., Malinovska, L., Nüske, E., Poser, I., Richter, D., and Alberti, S. (2015) Promiscuous interactions and protein disaggregases determine the material state of stress-inducible RNP granules. *Elife* **4,** e06807 CrossRef Medline
42. Park, Y. N., Zhao, X., Yim, Y. I., Todor, H., Ellerbrock, R., Reidy, M., Eisenberg, E., Masison, D. C., and Greene, L. E. (2014) Hsp104 overexpression cures *Saccharomyces cerevisiae* [PSI$^+$] by causing dissolution of the prion seeds. *Eukaryot. Cell* **13,** 635–647 CrossRef Medline
43. Parsell, D. A., Kowal, A. S., Singer, M. A., and Lindquist, S. (1994) Protein disaggregation mediated by heat-shock protein Hsp104. *Nature* **372,** 475–478 CrossRef Medline
44. Pei, F., DiSalvo, S., Sindi, S. S., and Serio, T. R. (2017) A dominant-negative mutant inhibits multiple prion variants through a common mechanism. *PLoS Genet.* **13,** e1007085 CrossRef Medline
45. Shorter, J., and Lindquist, S. (2004) Hsp104 catalyzes formation and elimination of self-replicating Sup35 prion conformers. *Science* **304,** 1793–1797 CrossRef Medline
46. Shorter, J., and Lindquist, S. (2008) Hsp104, Hsp70 and Hsp40 interplay regulates formation, growth and elimination of Sup35 prions. *EMBO J.* **27,** 2712–2724 CrossRef Medline
47. Sweeny, E. A., Jackrel, M. E., Go, M. S., Sochor, M. A., Razzo, B. M., DeSantis, M. E., Gupta, K., and Shorter, J. (2015) The Hsp104 N-terminal domain enables disaggregase plasticity and potentiation. *Mol. Cell* **57,** 836–849 CrossRef Medline
48. Wallace, E. W., Kear-Scott, J. L., Pilipenko, E. V., Schwartz, M. H., Laskowski, P. R., Rojek, A. E., Katanski, C. D., Riback, J. A., Dion, M. F., Franks, A. M., Airoldi, E. M., Pan, T., Budnik, B. A., and Drummond, D. A. (2015) Reversible, specific, active aggregates of endogenous proteins assemble upon heat stress. *Cell* **162,** 1286–1298 CrossRef Medline
49. Zhao, X., Rodriguez, R., Silberman, R. E., Ahearn, J. M., Saidha, S., Cummins, K. C., Eisenberg, E., and Greene, L. E. (2017) Heat shock protein 104 (Hsp104)-mediated curing of [PSI$^+$] yeast prions depends on both [PSI$^+$] conformation and the properties of the Hsp104 homologs. *J. Biol. Chem.* **292,** 8630–8641 CrossRef Medline
50. Shorter, J., and Southworth, D. R. (2019) Spiraling in control: structures and mechanisms of the Hsp104 disaggregase. *Cold Spring Harb. Perspect. Biol.*, pii: a034033, in press CrossRef Medline
51. Shorter, J., and Lindquist, S. (2006) Destruction or potentiation of different prions catalyzed by similar Hsp104 remodeling activities. *Mol. Cell* **23,** 425–438 CrossRef Medline
52. Jackrel, M. E., and Shorter, J. (2015) Engineering enhanced protein disaggregases for neurodegenerative disease. *Prion* **9,** 90–109 CrossRef Medline

53. Jackrel, M. E., and Shorter, J. (2014) Reversing deleterious protein aggregation with re-engineered protein disaggregases. *Cell Cycle* **13,** 1379–1383 CrossRef Medline
54. Lo Bianco, C., Shorter, J., Régulier, E., Lashuel, H., Iwatsubo, T., Lindquist, S., and Aebischer, P. (2008) Hsp104 antagonizes α-synuclein aggregation and reduces dopaminergic degeneration in a rat model of Parkinson disease. *J. Clin. Investig.* **118,** 3087–3097 CrossRef Medline
55. DeSantis, M. E., Leung, E. H., Sweeny, E. A., Jackrel, M. E., Cushman-Nick, M., Neuhaus-Follini, A., Vashist, S., Sochor, M. A., Knight, M. N., and Shorter, J. (2012) Operational plasticity enables hsp104 to disaggregate diverse amyloid and nonamyloid clients. *Cell* **151,** 778–793 CrossRef Medline
56. Mack, K. L., and Shorter, J. (2016) Engineering and evolution of molecular chaperones and protein disaggregases with enhanced activity. *Front. Mol. Biosci.* **3,** 8 CrossRef Medline
57. Jackrel, M. E., Tariq, A., Yee, K., Weitzman, R., and Shorter, J. (2014) Isolating potentiated Hsp104 variants using yeast proteinopathy models. *J. Vis. Exp.* e52089 CrossRef Medline
58. Jackrel, M. E., Yee, K., Tariq, A., Chen, A. I., and Shorter, J. (2015) Disparate mutations confer therapeutic gain of Hsp104 function. *ACS Chem. Biol.* **10,** 2672–2679 CrossRef Medline
59. Torrente, M. P., Chuang, E., Noll, M. M., Jackrel, M. E., Go, M. S., and Shorter, J. (2016) Mechanistic insights into Hsp104 potentiation. *J. Biol. Chem.* **291,** 5101–5115 CrossRef Medline
60. Tariq, A., Lin, J., Noll, M. M., Torrente, M. P., Mack, K. L., Murillo, O. H., Jackrel, M. E., and Shorter, J. (2018) Potentiating Hsp104 activity via phosphomimetic mutations in the middle domain. *FEMS Yeast Res.* **18,** foy042 CrossRef Medline
61. Lindberg, I., Shorter, J., Wiseman, R. L., Chiti, F., Dickey, C. A., and McLean, P. J. (2015) Chaperones in neurodegeneration. *J. Neurosci.* **35,** 13853–13859 CrossRef Medline
62. Thelin-Järnum, S., Göransson, M., Burguete, A. S., Olofsson, A., and Aman, P. (2002) The myxoid liposarcoma specific TLS-CHOP fusion protein localizes to nuclear structures distinct from PML nuclear bodies. *Int. J. Cancer* **97,** 446–450 CrossRef Medline
63. Göransson, M., Wedin, M., and Aman, P. (2002) Temperature-dependent localization of TLS-CHOP to splicing factor compartments. *Exp. Cell Res.* **278,** 125–132 CrossRef Medline
64. Burke, K. A., Janke, A. M., Rhine, C. L., and Fawzi, N. L. (2015) Residue-by-residue view of *in vitro* FUS granules that bind the C-terminal domain of RNA polymerase II. *Mol. Cell* **60,** 231–241 CrossRef Medline
65. Daigle, J. G., Lanson, N. A., Jr., Smith, R. B., Casci, I., Maltare, A., Monaghan, J., Nichols, C. D., Kryndushkin, D., Shewmaker, F., and Pandey, U. B. (2013) RNA-binding ability of FUS regulates neurodegeneration, cytoplasmic mislocalization and incorporation into stress granules associated with FUS carrying ALS-linked mutations. *Hum. Mol. Genet.* **22,** 1193–1205 CrossRef Medline
66. Bogaert, E., Boeynaems, S., Kato, M., Guo, L., Caulfield, T. R., Steyaert, J., Scheveneels, W., Wilmans, N., Haeck, W., Hersmus, N., Schymkowitz, J., Rousseau, F., Shorter, J., Callaerts, P., Robberecht, W., *et al.* (2018) Molecular dissection of FUS points at synergistic effect of low-complexity domains in toxicity. *Cell Rep.* **24,** 529–537.e4 CrossRef Medline
67. Guo, L., and Shorter, J. (2017) Biology and pathobiology of TDP-43 and emergent therapeutic strategies. *Cold Spring Harb. Perspect. Med.* **7,** a024554 CrossRef Medline
68. Voigt, A., Herholz, D., Fiesel, F. C., Kaur, K., Müller, D., Karsten, P., Weber, S. S., Kahle, P. J., Marquardt, T., and Schulz, J. B. (2010) TDP-43-mediated neuron loss *in vivo* requires RNA-binding activity. *PLoS One* **5,** e12247 CrossRef Medline
69. Flores, B. N., Li, X., Malik, A. M., Martinez, J., Beg, A. A., and Barmada, S. J. (2019) An intramolecular salt bridge linking TDP43 RNA binding, protein stability, and TDP43-dependent neurodegeneration. *Cell Rep.* **27,** 1133–1150.e8 CrossRef Medline
70. Neumann, M., Bentmann, E., Dormann, D., Jawaid, A., DeJesus-Hernandez, M., Ansorge, O., Roeber, S., Kretzschmar, H. A., Munoz, D. G., Kusaka, H., Yokota, O., Ang, L. C., Bilbao, J., Rademakers, R., Haass, C., *et al.* (2011) FET proteins TAF15 and EWS are selective markers that distinguish FTLD with FUS pathology from amyotrophic lateral sclerosis with FUS mutations. *Brain* **134,** 2595–2609 CrossRef Medline
71. Neumann, M., Valori, C. F., Ansorge, O., Kretzschmar, H. A., Munoz, D. G., Kusaka, H., Yokota, O., Ishihara, K., Ang, L. C., Bilbao, J. M., and Mackenzie, I. R. (2012) Transportin 1 accumulates specifically with FET proteins but no other transportin cargos in FTLD-FUS and is absent in FUS inclusions in ALS with FUS mutations. *Acta Neuropathol.* **124,** 705–716 CrossRef Medline
72. Shin, Y., and Brangwynne, C. P. (2017) Liquid phase condensation in cell physiology and disease. *Science* **357,** eaaf4382 CrossRef Medline
73. Gates, S. N., Yokom, A. L., Lin, J., Jackrel, M. E., Rizo, A. N., Kendsersky, N. M., Buell, C. E., Sweeny, E. A., Mack, K. L., Chuang, E., Torrente, M. P., Su, M., Shorter, J., and Southworth, D. R. (2017) Ratchet-like polypeptide translocation mechanism of the AAA+ disaggregase Hsp104. *Science* **357,** 273–279 CrossRef Medline
74. Yokom, A. L., Gates, S. N., Jackrel, M. E., Mack, K. L., Su, M., Shorter, J., and Southworth, D. R. (2016) Spiral architecture of the Hsp104 disaggregase reveals the basis for polypeptide translocation. *Nat. Struct. Mol. Biol.* **23,** 830–837 CrossRef Medline
75. Tkach, J. M., and Glover, J. R. (2008) Nucleocytoplasmic trafficking of the molecular chaperone Hsp104 in unstressed and heat-shocked cells. *Traffic* **9,** 39–56 CrossRef Medline
76. Kroschwald, S., Munder, M. C., Maharana, S., Franzmann, T. M., Richter, D., Ruer, M., Hyman, A. A., and Alberti, S. (2018) Different material states of Pub1 condensates define distinct modes of stress adaptation and recovery. *Cell Rep.* **23,** 3327–3339 CrossRef Medline
77. Krobitsch, S., and Lindquist, S. (2000) Aggregation of huntingtin in yeast varies with the length of the polyglutamine expansion and the expression of chaperone proteins. *Proc. Natl. Acad. Sci. U.S.A.* **97,** 1589–1594 CrossRef Medline
78. Jovičić, A., Mertens, J., Boeynaems, S., Bogaert, E., Chai, N., Yamada, S. B., Paul, J. W., 3rd, Sun, S., Herdy, J. R., Bieri, G., Kramer, N. J., Gage, F. H., Van Den Bosch, L., Robberecht, W., and Gitler, A. D. (2015) Modifiers of C9orf72 dipeptide repeat toxicity connect nucleocytoplasmic transport defects to FTD/ALS. *Nat. Neurosci.* **18,** 1226–1229 CrossRef Medline
79. Gitler, A. D., Dhillon, P., and Shorter, J. (2017) Neurodegenerative disease: models, mechanisms, and a new hope. *Dis. Model. Mech.* **10,** 499–502 CrossRef Medline
80. Sweeny, E. A., and Shorter, J. (2016) Mechanistic and structural insights into the prion-disaggregase activity of Hsp104. *J. Mol. Biol.* **428,** 1870–1885 CrossRef Medline
81. Sanchez, Y., and Lindquist, S. L. (1990) HSP104 required for induced thermotolerance. *Science* **248,** 1112–1115 CrossRef Medline
82. Gietz, R. D., and Schiestl, R. H. (2007) High-efficiency yeast transformation using the LiAc/SS carrier DNA/PEG method. *Nat. Protoc.* **2,** 31–34 CrossRef Medline